AIP Applied Physics Letters

# Engineering the composition, morphology, and optical properties of InAsSb nanostructures via graded growth technique

W. Lei, H. H. Tan, and C. Jagadish

Citation: Appl. Phys. Lett. **102**, 033111 (2013); doi: 10.1063/1.4789513
View online: http://dx.doi.org/10.1063/1.4789513
View Table of Contents: http://apl.aip.org/resource/1/APPLAB/v102/i3
Published by the American Institute of Physics.

## Additional information on Appl. Phys. Lett.

Journal Homepage: http://apl.aip.org/
Journal Information: http://apl.aip.org/about/about_the_journal
Top downloads: http://apl.aip.org/features/most_downloaded
Information for Authors: http://apl.aip.org/authors

ADVERTISEMENT

Downloaded 10 Apr 2013 to 150.203.178.118. This article is copyrighted as indicated in the abstract. Reuse of AIP content is subject to the terms at: http://apl.aip.org/about/rights_and_permissions

APPLIED PHYSICS LETTERS **102**, 033111 (2013)

# Engineering the composition, morphology, and optical properties of InAsSb nanostructures *via* graded growth technique

W. Lei,[1,2,a)] H. H. Tan,[1] and C. Jagadish[1]
[1]*Department of Electronic Materials Engineering, Research School of Physics and Engineering, The Australian National University, Canberra, ACT 0200, Australia*
[2]*School of Electrical, Electronic and Computer Engineering, The University of Western Australia, Crawley 6009, WA, Australia*

(Received 23 October 2012; accepted 14 January 2013; published online 25 January 2013)

Graded growth technique is utilized to realize the control over the composition, morphology, and optical properties of self-assembled InAsSb/InGaAs/InP nanostructures. By increasing the initial mole fraction of the Sb precursor during the graded growth of InAsSb, more Sb atoms can be incorporated into the InAsSb nanostructures despite the same Sb mole fraction averaged over the graded growth. This leads to a shape change from dots to dashes/wires for the InAsSb nanostructures. As a result of the composition and morphology change, photoluminescence from the InAsSb nanostructures shows different polarization and temperature characteristics. This work demonstrates a technologically important technique—graded growth, to control the growth and the resultant physical properties of self-assembled semiconductor nanostructures. © *2013 American Institute of Physics*. [http://dx.doi.org/10.1063/1.4789513]

Semiconductor nanostructures such as quantum dots and quantum wires attract much attention recently due to their potential applications in devices and the interest in fundamental study.[1] For example, In(Ga)As quantum dots on both GaAs and InP substrates have been studied for the applications in 1.3 $\mu$m and 1.55 $\mu$m optical communication lasers in the last two decades.[2–5] Most of these semiconductor nanostructures are fabricated through epitaxial growth techniques such as molecular beam epitaxy and metal-organic chemical vapour deposition *via* the Stranski–Krastanov mode, where the nanostructures are formed by releasing the strain energy (lattice mismatch) accumulated in the system when the thickness of the epitaxial layer exceeds a critical value.[1–5] Furthermore, during the growth of these nanostructures, group V atoms are usually introduced into the growth chamber simultaneously with group III atoms at a constant flux or mole flow. By engineering the growth conditions like growth temperature, growth rate, V/III ratio, strain field, and buffer layer, the morphology and physical properties of the nanostructures can be changed significantly.[3,6,7] Because of the different sticking coefficients and incorporation efficiencies of different atoms, graded growth provides another interesting approach to engineer not only the morphology and physical properties but also the composition of ternary and quaternary semiconductor alloys and their nanostructures. However, this graded growth technique is seldom studied, especially for the semiconductor alloys with two different group V elements. In this work, graded growth technique is applied in the epitaxial growth of InAsSb ternary nanostructures to engineer their composition, morphology, and physical properties. These nanostructures have potential applications in mid-infrared optoelectronic devices.[8–12] It is found that by using different graded approaches the actual Sb composition in InAsSb nanostructures can be changed significantly despite the fact that their nominal Sb mole fraction (averaged over the graded growth) is kept the same, which results in different morphologies for the InAsSb nanostructures. As a result of their composition and morphological changes, photoluminescence from these InAsSb nanostructures shows different polarization and temperature characteristics.

The InAsSb nanostructures were grown on semi-insulating InP (001) substrates in a horizontal-flow metal-organic chemical vapor deposition reactor (AIX200/4) at a pressure of 180 mbar. Trimethylindium (TMIn), trimethylgallium (TMGa), trimethylantimony (TMSb), $PH_3$, and $AsH_3$ were used as the precursors and ultra-high purity $H_2$ as the carrier gas. The InAsSb nanostructures were grown using the following layer sequence: First, a 50 nm InP layer and 100 nm $In_{0.53}Ga_{0.47}As$ layer were deposited at 650 °C, then the temperature was dropped to 480 °C to grow 4 monolayers (MLs) of $InAs_xSb_{1-x}$ nanostructures which was immediately capped with 8 nm $In_{0.53}Ga_{0.47}As$ without any growth interruption. After that the temperature was ramped up to 650 °C and a further 100 nm $In_{0.53}Ga_{0.47}As$ layer was deposited. The same steps were followed to grow a top layer of $InAs_xSb_{1-x}$ nanostructures for atomic force microscopy (AFM) measurements. For the growth of 4 ML of InAsSb in all samples, a constant TMIn flow ($2.011 \times 10^{-5}$ moles/min) was introduced into the growth chamber for 8 s simultaneously with $AsH_3$ and TMSb flows based on the assumption that the growth rate of InAsSb layers is only dependent on the TMIn flow rate. To engineer the composition, morphology, and physical properties of the InAsSb nanostructures, five different graded growth approaches were used during the growth of InAsSb, and the corresponding samples were named as samples A, B, C, D, and E, as shown Figure 1(a). For all the graded growths, the $AsH_3$ and TMSb mole fraction were varied linearly from the initial to the final values as illustrated in Figure 1(a). The morphology of the top InAsSb nanostructures was characterized by using AFM in tapping mode. To determine the actual As and Sb composition in the InAsSb

a)Electronic addresses: wen.lei@anu.edu.au and wen.lei@uwa.edu.au.

 © 2013 American Institute of Physics

Downloaded 10 Apr 2013 to 150.203.178.118. This article is copyrighted as indicated in the abstract. Reuse of AIP content is subject to the terms at: http://apl.aip.org/about/rights_and_permissions

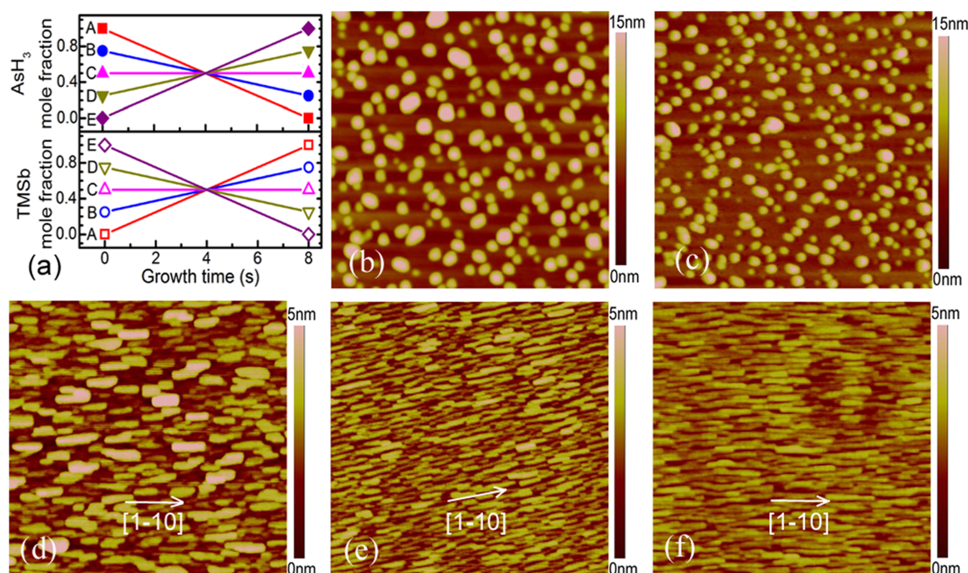


FIG. 1. Sketched graded growth processes (a) and AFM images of InAsSb nanostructures in samples A (b), B (c), C (d), D (e), and E (f).

islands, Raman scattering measurements were performed on all the samples in backscattering geometry at room temperature with a Renishaw 2000 confocal micro-Raman system, where $z(x', x'+y')\bar{z}$ polarization configuration ($x\|[100]$, $y\|[010]$, $z\|[001]$, $x'\|[110]$, $\|y'\|[1\bar{1}0]$) was used. The samples were excited by the 632.8 nm line of a He-Ne laser to a 2 $\mu$m spot on the surface with an excitation power of 4 mW. Photoluminescence (PL) measurements were carried out under excitation by a 532 nm laser diode. The luminescence signal was collected by a liquid nitrogen-cooled extended InGaAs photodetector through a 0.5 m monochromator.

Figures 1(b)–1(f) show the AFM images of the InAsSb nanostructures in samples A, B, C, D, and E. The InAsSb nanostructures in samples A and B show dot-like morphology, while those in sample C, D, and E show dash- and wire-like morphology. Except for a few large dislocated islands, the quantum dots have an average height of ~7 and 6 nm and an average diameter of ~55 and 50 nm for samples A and B, respectively. Compared with the dots in sample A, the dots in sample B have a slightly elongated shape, the reason for which will be discussed later. In contrast, the InAsSb dashes/wires have an average height of ~3.5, 2.5, and 2 nm, an average lateral width (along the [110] direction) of ~35, 20, and 22 nm, and an average length (along the $[1\bar{1}0]$ direction) of ~104, 130, and 190 nm for samples C, D, and E, respectively. More interestingly, the island shape suddenly changes from dot into dash when the initial mole fraction of Sb precursor (TMSb) during the graded growth increases from 25% to 50%. This sudden morphological change is very similar to what was observed in one of our previous works about the effect of Sb exposure on the morphology of InAsSb nanostructures.[13] As discussed in Ref. 13, a higher Sb composition in InAsSb nanostructures will cause a larger lattice mismatch between InAsSb and substrate/buffer layer and thus a larger strain in the system. This will induce a smaller critical size $e\alpha_0$ for the island's shape change in the system and thus lead to a shape change from dots to dashes/wires once the island's size surpasses the critical size $e\alpha_0$, which might also be the reason for the morphological changes observed here.

To confirm the change of the actual Sb composition in InAsSb nanostructures, Raman spectroscopy was performed on all the samples. Figure 2 shows the Raman spectra of sample A, B, C, D, and E, respectively. Clearly, four Raman peaks are observed for all the samples, where the peaks around 229.6, 245.2, and 349.4 $cm^{-1}$ can be attributed to the InAs-like TO, InAs-like LO, and InP LO phonon modes, respectively.[13–15] However, there is another Raman peak centred around 257.9–265.7 $cm^{-1}$, which can be assigned to the phonon mode of the InAsSb nanostructures.[14,15] Generally, for a perfect heterostructure, both compressive strain (upward shift) and confinement effects (downward shift) play a dominant role in the phonon frequency shift ($\Delta\omega_{exp}$): ($\Delta\omega_{exp} = \Delta\omega_{strain} + \Delta\omega_c$).[16,17] When the initial TMSb mole fraction during the graded growth increases from 0 to 1, the island height decreases from 7 to 2 nm, suggesting a certain increase of phonon confinement effect in the islands and thus a downward frequency shift (~1.3 $cm^{-1}$ for $InAs_{0.5}Sb_{0.5}$ islands according to the modified spatial correlation model[18,19]). However, this frequency shift is quite small compared with the large net frequency shift ($\geq$13 $cm^{-1}$) relative to the InAs LO mode (245 $cm^{-1}$). This indicates that

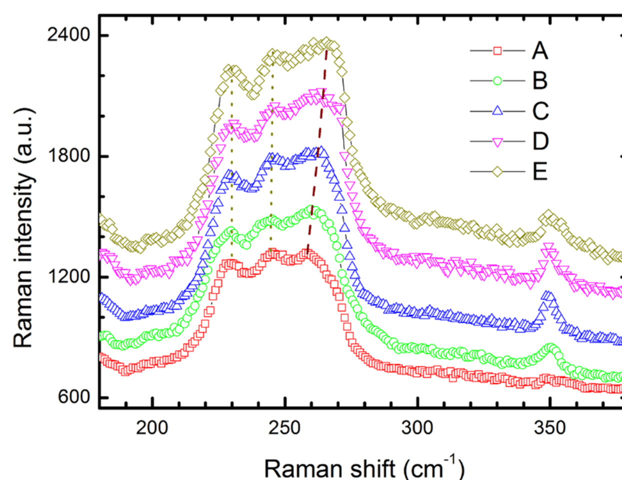


FIG. 2. Raman spectra of samples A, B, C, D, and E.

Downloaded 10 Apr 2013 to 150.203.178.118. This article is copyrighted as indicated in the abstract. Reuse of AIP content is subject to the terms at: http://apl.aip.org/about/rights_and_permissions

the Raman shift here is mainly dominated by the compressive strain in the InAsSb nanostructures. With increasing the initial TMSb mole fraction from 0 to 1, the compressive strain in the InAsSb islands increases significantly (the phonon frequency shift from 257.9 to 259.8, to 261.8, to 263.7, and to 265.7 $cm^{-1}$ corresponds to an increase of compressive strain from 4.0% to 4.6%, to 5.2%, to 6%, and to 6.8% for the islands according to the model and parameters reported in Refs. 16, 17, and 20) and induces an upward frequency shift far surpassing the downward frequency shift caused by phonon confinement effect. As reported in Ref. 13, the compressive strain in InAsSb nanostructures is mainly determined by the lattice mismatch between the substrate and InAsSb. Therefore, the actual average Sb composition in InAsSb nanostructures can be estimated to be 0.11, 0.2, 0.28, 0.39, and 0.5 for sample A, B, C, D, and E, respectively. Because In-As bond is stronger than In-Sb bond,[21] it is relatively easier for As atoms to be incorporated into the InAsSb nanostructures compared with Sb atoms. But a higher initial TMSb mole fraction during the graded growth like that in sample E will increase the driving force for more Sb atoms to be incorporated into InAsSb islands, leading to a higher actual average Sb composition in InAsSb nanostructures and thus a significant increase of the compressive strain. This suggests that the initial TMSb mole fraction during the graded growth plays an important role in controlling the actual Sb composition in InAsSb nanostructures.

As a result of the morphology and composition changes, the InAsSb nanostructures exhibit different emission wavelength and different optical polarization characteristics. Figure 3 shows the 77 K PL spectra and emission polarization features of samples A, B, C, D, and E. It is observed that the PL peak shifts from 1840 nm (A) to 1826 nm (B), to 1762 nm (C), 1765 nm (D), and to 1785 nm (E) as the initial TMSb mole fraction increases from 0 to 1. This shift of PL peak position with increasing initial TMSb mole fraction can be attributed to the change of island size and actual average Sb composition. The inset of Figure 3 shows the polar scan of PL intensity of the samples. Obviously, the optical anisotropy of the InAsSb islands increases as the initial TMSb mole fraction increases, especially as the initial TMSb mole fraction increases from 0.25 to 0.5, which is mainly caused by their shape anisotropy despite strain having some influence.

To further study the influence of the graded growth on the optical properties of InAsSb nanostructures, temperature dependent PL measurements were performed. Figure 4 shows the PL peak energy and intensity as a function of temperature for sample A, B, C, D, and E. All the samples show a faster red-shift for their PL peaks with increasing temperature compared with bulk InAs or InSb, which is expected for low-dimensional structures such as quantum dots and quantum dashes. Interestingly, the red shift rate of the PL peak decreases with increasing the initial TMSb mole fraction during the graded growth, especially when the initial TMSb mole fraction increases from 0.25 to 0.5. This change of red shift rate might be due to the increase of actual average Sb composition in InAsSb nanostructures with increasing the initial TMSb mole fraction during the graded growth. A similar change of red shift rate with increasing the Sb composition was observed before for $InAs_{1-x}Sb_x$ epitaxial layers on GaAs and InAs substrates.[22–24] The exact reason for this change of red shift rate is still not very clear though some suggestions were proposed such as emission involving impurity state, free carrier transition, and wave-vector-nonconserving transition,[22–24] which remains to be studied later. As for the difference among the red-shift rate of samples C, D, and E, the different energy barriers for carrier escape might also play a role. For example, the InAsSb nanostructures in

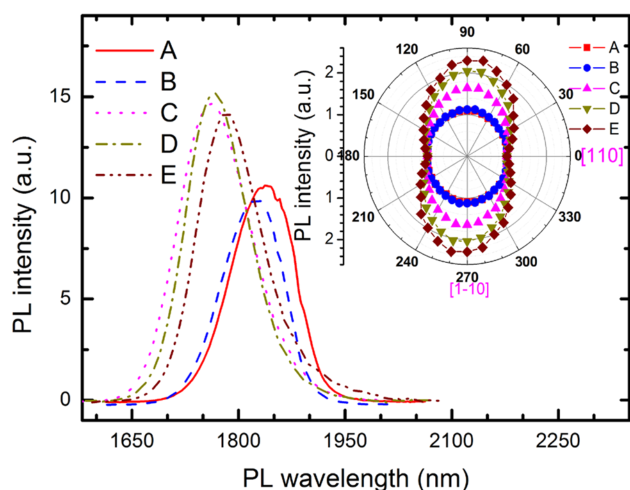


FIG. 3. 77 K PL spectra and 77 K polar scan of the PL intensity of samples A, B, C, D, and E.

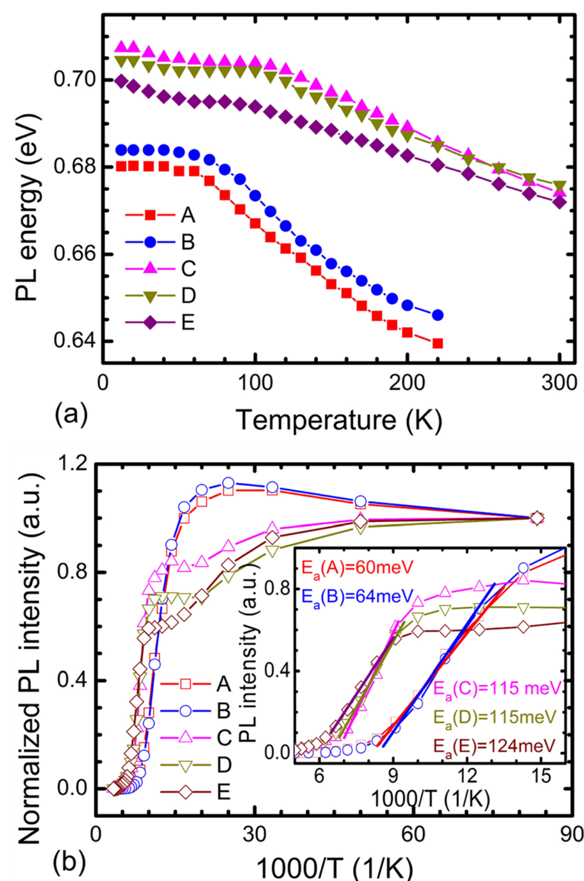


FIG. 4. Temperature dependent PL energy (a) and PL intensity (b) of samples A, B, C, D, and E. The inset of (b) shows the fitting of thermal excitation energy through the PL intensity quenching at high temperatures.

Downloaded 10 Apr 2013 to 150.203.178.118. This article is copyrighted as indicated in the abstract. Reuse of AIP content is subject to the terms at: http://apl.aip.org/about/rights_and_permissions

sample E have the lowest bandgap and thus the largest energy barrier for carrier escape, leading to the smallest red-shift rate for the PL peak. By fitting the PL intensity at higher temperatures, the carrier excitation energy ($E_a$) can be obtained,[25,26] which is estimated to be around 60, 64, 115, 115, and 124 meV for samples A, B, C, D, and E, respectively. It is interesting to observe that although the PL energies of samples A and B are only slightly smaller than those of samples C, D, and E, the $E_a$ values of samples A and B are significantly smaller than those of samples C, D, and E. This is mainly caused by the dislocated InAsSb islands observed in samples A and B which can act as non-radiative recombination centers. The $E_a$ values of sample C, D, and E suggest that the thermal escape of carriers in sample C, D, and E at high temperatures is mainly dominated by the bipolar thermal escape process (both electrons and holes) considering the bandgap of InGaAs (0.82 eV at 77 K) and the PL energies of InAsSb nanostructures measured. It should be mentioned that the PL peak energy and PL intensity of samples C, D, and E present a "S-shape" temperature dependence, as shown in Figure 4.[27] This "S-shape" temperature dependence is mainly caused by the significant thermal redistribution of localized carriers among the InAsSb islands in these samples due to the higher island density and thus smaller distance among the islands in sample C, D, and E compared with those in samples A and B.

In summary, graded growth is used to realize the control over the composition, morphology, and physical properties of semiconductor InAsSb ternary alloy nanostructures. A higher initial mole fraction of TMSb during the graded growth can lead to a higher actual average Sb composition in InAsSb islands. As a result of the composition change, the InAsSb nanostructures present different morphologies and optical properties, which will be useful for making devices with different emission characteristics.

Financial support from Australian Research Council is gratefully acknowledged. Facilities used in this work are supported by the Australian National Fabrication Facility.

[1] D. Bimberg, M. Grundmann, and N. N. Ledentsov, *Quantum Dot Heterostructures* (Wiley, New York, 1999).
[2] H. Liu, T. Wang, Q. Jiang, R. Hogg, F. Tutu, F. Pozzi, and A. Seeds, Nat. Photonics **5**, 416 (2011).
[3] C. Zhao, Y. H. Chen, C. X. Cui, B. Xu, J. Sun, W. Lei, L. K. Lu, and Z. G. Wang, J. Chem. Phys. **123**, 094708 (2005).
[4] E. S. Semenova, I. V. Kulkova, S. Kadkhodazadeh, M. Schubert, and K. Yvind, Appl. Phys. Lett. **99**, 101106 (2011).
[5] X.-Q. Huang, F.-Q. Liu, X.-L. Che, J.-Q. Liu, W. Lei, and Z.-G. Wang, J. Cryst. Growth **270**, 364 (2004).
[6] W. Lei, H. H. Tan, and C. Jagadish, Appl. Phys. Lett. **95**, 013108 (2009).
[7] W. Lei, H. H. Tan, and C. Jagadish, Appl. Phys. Lett. **95**, 143124 (2009).
[8] Y. Qiu and D. Uhl, Appl. Phys. Lett. **84**, 1510 (2004).
[9] F. Doré, C. Cornet, A. Schliwa, A. Ballestar, J. Even, N. Bertru, O. Dehaese, I. Alghoraibi, H. Folliot, R. Piron, A. Le Corre, and S. Loualiche, Phys. Status Solidi C **3**, 524 (2006).
[10] W. Lei and C. Jagadish, J. Appl. Phys. **104**, 091101 (2008).
[11] W. Lei, H. H. Tan, and C. Jagadish, J. Phys. D: Appl. Phys. **43**, 302001 (2010).
[12] X. H. Tang, B. L. Zhang, and Z. Y. Yin, Cryst. Eng. Comm. **15**, 604 (2013).
[13] W. Lei, H. H. Tan, and C. Jagadish, Appl. Phys. Lett. **99**, 193110 (2011).
[14] W. Lei, Y. H. Chen, B. Xu, X. L. Ye, Y. P. Zeng, and Z. G. Wang, Nanotechnology **16**, 1974 (2005).
[15] W. Lei, H. H. Tan, C. Jagadish, Q. J. Ren, J. Lu, and Z. H. Chen, Appl. Phys. Lett. **97**, 223108 (2010).
[16] I. Rasnik, M. J. S. P. Brasil, F. Cerdeira, C. A. C. Mendonca, and M. A. Cotta, J. Appl. Phys. **87**, 1165 (2000).
[17] B. Jusserand and M. Cardona, in *Light Scattering in Solids V: Topics in Applied Physics*, edited by M. Cardona and G. Güntherodt (Springer, Heidelburg, 1989), Vol. 66, pp. 124–128.
[18] H. Richter, Z. P. Wang, and L. Ley, Solid State Commun. **39**, 625 (1981).
[19] I. H. Campbell and P. M. Fauchet, Solid State Commun. **58**, 739 (1986).
[20] R. Carles, V. Saint-Cricq, J. B. Renucci, M. A. Renucci, and A. Zwick, Phys. Rev. B **22**, 4804 (1980).
[21] G. B. Stringfellow, *Organometallic Vapor-Phase Epitaxy: Theory and Practice* (Academic, San Diego, California, 1999), p. 83.
[22] M. Y. Yen, R. People, K. W. Wecht, and A. Y. Cho, Appl. Phys. Lett. **52**, 489 (1988).
[23] M. Y. Yen, R. People, and K. W. Wecht, J. Appl. Phys. **64**, 952 (1988).
[24] Z. M. Fang, K. Y. Ma, D. H. Jaw, R. M. Cohen, and G. B. Stringfellow, J. Appl. Phys. **67**, 7034 (1990).
[25] W. Lei, Y. H. Chen, Y. L. Wang, X. Q. Huang, Ch. Zhao, J. Q. Liu, B. Xu, P. Jin, Y. P. Zeng, and Z. G. Wang, J. Cryst. Growth **286**, 23 (2006).
[26] Y. T. Dai, J. C. Fan, Y. F. Chen, R. M. Lin, S. C. Lee, and H. H. Lin, J. Appl. Phys. **82**, 4489 (1997).
[27] Q. Li, S. J. Xu, M. H. Xie, and S. Y. Tong, Europhys. Lett. **71**, 994 (2005).

Downloaded 10 Apr 2013 to 150.203.178.118. This article is copyrighted as indicated in the abstract. Reuse of AIP content is subject to the terms at: http://apl.aip.org/about/rights_and_permissions